Adaptation of Class-13 α-Amylases to Diverse Living Conditions

Anni Linden and Matthias Wilmanns*[a]

*There are currently 35 available nonredundant molecular structures of class-13 α-amylases (EC 3.2.1.1), mostly from microbial organisms living under a wide range of environmental conditions. One of the most recent additions has been the first α-amylase structure of a hyperthermophilic archaeon [Linden et al., J. Biol. Chem. **2003**, 278, 9875–9884]. The structure has been used for comparative analyses with a representative set of three α-amylases from thermophilic, mesophilic and psychrophilic sources to identify molecular parameters for environmental adaptation. Our analysis supports generally observed trends such as an increase in structural compactness as well as an increase in salt bridges in order to cope with high-temperature conditions. The two representative thermophilic structures used in this comparative study have independently evolved di-metal centres—not present in the mesophilic and psychrophilic structures—in the vicinity of the active site. These observations may provide impetus for the design of α-amylases with improved molecular properties to enhance their utility in biotechnological processes.*

Introduction

The categorisation of archaea as the third domain of life, the first two being bacteria and eukarya,[1, 2] has dramatically changed the classification scheme of microorganisms. The extreme environmental habitats of members of the archaea domain and their apparent closer relation to eukaryotes than to bacteria has sparked much interest in the isolation and study of these organisms. These extreme conditions include high temperatures and extremes of pH, redox potential and salinity. Several hyperthermophilic archaea and bacteria that grow at temperatures above 80 °C have been isolated and characterised.[3] In order to contend with, and possibly to take advantage of, such extremely high growth temperatures, these organisms have evolved mechanisms for increased intrinsic thermostability of cellular components such as proteins and nucleic acids. Some of the enzymes originating from organisms living under extreme environmental conditions exhibit remarkable stability against detergents and proteolytic digestion,[4, 5] making them potential targets for industrial applications such as the polymerase chain reaction (PCR) or in the food and textile industries.[6–10] As such, there has ensued intense interest in the identification of factors influencing the thermostability of proteins, with the potential to enhance our understanding of the evolutionary adaptations to specific environmental conditions.

One of the most important tools used to investigate the molecular basis of protein thermostability is direct comparison of the molecular structures of corresponding proteins from different organisms, thereby allowing attributions of measured differences to environment adaptations rather than to differences in function. The increasing availability of X-ray structures of proteins from extremophilic organisms, ranging from psychrophilic to hyperthermophilic living conditions, has allowed several comparative studies to infer the contributions of different factors to thermostability by computational, genetic engineering and a variety of biophysical methods.[11, 12] Numerous attempts to provide statistical models to uncover the significance of observed property changes have been made.[13–16] With the aid of these criteria, the search is underway to assess molecular parameters—such as the frequency of salt bridges, surface polarity and structural compactness—that generally undergo significant alterations in response to specific environmental conditions.[14] Other quantifiable molecular parameters such as the presence of disulfide bridges, metal centres and oligomeric assemblies may differ with respect to their presence or absence in specific protein families.

Thanks to their widespread occurrence and potential application in large-scale biotechnology processes, class-13 α-amylases represent the most thoroughly studied family of proteins with respect to their function and structure.[17, 18] In this contribution we compare environmentally sensitive structural properties of a limited set of four members of this family. We use the recently determined crystal structure of the first archaeal α-amylase from the hyperthermophile *Pyrococcus woesei* as reference,[19] to extend previous comparative studies that focused on functional/structural data of the α-amylases from the psychrophile *Alteromonas haloplanctis*[20] and the hyperthermophilic bacteria *Bacillus licheniformis* and its mesophilic homologue *Bacillus amyloliquefaciens*.[21–23] A specific aim of this contribution is to identify α-amylase-specific adaptations to contend with hyperthermophilic conditions.

[a] *Dr. A. Linden, Dr. M. Wilmanns*
EMBL-Hamburg c/o DESY, Notkestrasse 85
22603 Hamburg (Germany)
Fax: (+49) 40-89902-149
E-mail: wilmanns@embl-hamburg.de

 DOI: 10.1002/cbic.200300734

Results and Discussion

Selection of α-amylase structures

According to a recent release of the Protein Data Bank (July 15, 2003; pdb.org) and the CAZY server (July 2003; afmb.cns-mfrss.fr/CAZY), there are currently 35 available nonredundant class-13 α-amylase structures, while there are 58 nonredundant α-amylase structures, including those from other classes. Thus, most of the known α-amylase structures belong to the class-13 family. These proteins share a common central catalytic $(\beta\alpha)_8$-barrel domain A, which is flanked by the two noncatalytic domains B and C. Since a comprehensive comparative structural analysis of all known α-amylase structures is beyond the scope of this contribution, we chose to restrict our analysis to a limited, yet representative set of four crystal structures that have been determined at resolutions of at least 2.0 Å. These are the α-amylase structures from the thermophile *Bacillus stearothermophilus* (BSTA, PDB: 1HVX), the mesophile *Hordeum vulgare* (HVA, PDB: 1AVA), and the psychrophile *Pseudoalteromonas haloplanctis* (PHA, PDB: 1G94). The recently solved structure of the α-amylase from *P. woesei* (PWA, PDB code: 1MXG) has been used as reference. These proteins are found in organisms that grow at temperatures ranging from less than 20 °C to 100 °C (Table 1). Their structures superimpose with a root mean square deviation of less than 2.5 Å and Q-scores (a function of the structural alignment that takes both the rms deviation and the alignment length into account) above 0.3 (Table 2). The corresponding structure-based alignment is shown in Figure 1. The structure of the hyperthermostable α-amylase from *B. licheniformis* (BLA, PDB: 1BLI), which is closely related to the BSTA structure, superimposes with a comparable Q-score. Therefore, most of the conclusions drawn from BSTA are also applicable to BLA. The following comparison focuses on surface/volume, salt bridges, disulfide bridges and metal centres found in these four structures.

Protein volume and surface

The amino acid sequences that form the visible portion of these four α-amylase structures range from 400 to 480 residues in length (Table 1). The overall volumes of their molecular structures are within the 35000 – 44000 Å^3 range and generally correlate with the sequence lengths (Table 3). However, the calculated surface/volume ratios of these structures reveal that the representative thermophilic structures (PWA, BSTA) are considerably more compact, by approximately 10%, than their mesophilic counterpart (HVA). Changes in the packing densities of these structures are amplified by the number of cavities within each structure (Table 4). For example, the mesophilic HVA structure contains almost twice as many cavities (52) as the hyperthermophilic PWA (28 cavities) one, accounting for about twice the fraction of the relative structural volume (HVA: 6.61%; PWA: 3.34%). In contrast with these results, the cold-adapted amylase (PHA) has fewer cavities than the thermophilic one (BSTA). Furthermore, comparison between PHA and its most structurally similar mesophilic counterparts does not show any significant differences in cavity volume,[16] indicating that there is no apparent correlation between the number and volume of cavities and thermostability throughout the family-13 glycoside hydrolases. In terms of surface distribution of polar and apolar atoms, the representative psychrophilic structure (PHA) appears to be an outlier, with 50% of surface atoms being polar, compared with 45 – 46% for those of the other three α-amylases. Support for these trends from similar results from other protein

Table 2. *Structural similarities.*

N_{algn} [$\%_{seq}$] Q-score rmsd [Å]	PWA	BSTA	HVA	PHA
PWA	–	376	336	324
	–	32	31	20
BSTA	0.46	–	347	337
	2.04	–	27	20
HVA	0.52	0.40	–	291
	1.43	2.11	–	20
PHA	0.33	0.32	0.31	–
	2.43	2.38	2.13	–

Table 3. *Accessible surface areas (ASAs) and volumes.*

Enzyme	Total ASA [Å^2]	Polar ASA [Å^2, %]	Total volume [Å^3]	Surface/volume [Å^{-1}]
PWA	15947	7331(46)	39941	0.40
BSTA	17519	8050(46)	43615	0.40
HVA	15002	6692(45)	35601	0.45
PHA	16475	8245(50)	38686	0.43

Table 1. *Properties of α-amylases used for comparison.*

Enzyme acronym *Source*	PWA *P. woesei*	BSTA *B. stearothermophilus*	HVA *H. vulgare*	PHA *P. haloplanctis*
Thermostability				
optimum growth of source [°C]:	97 – 100	55	24	20 – 25
enzyme stability	Stable at 98 °C[34]	$T_{1/2}$ (90 °C): 50 min[37]	$T_{1/2}$ (60 °C): 26 min[48]	$T_m = 44$ °C[49]
classification	hyperthermophile	thermophile	mesophile	psychrophile
Structural parameters				
PDB code	1MXG	1HVX	1AVA	1G94
no. residues	435	483	403	448
resolution [Å]	1.60	2.00	1.90	1.74

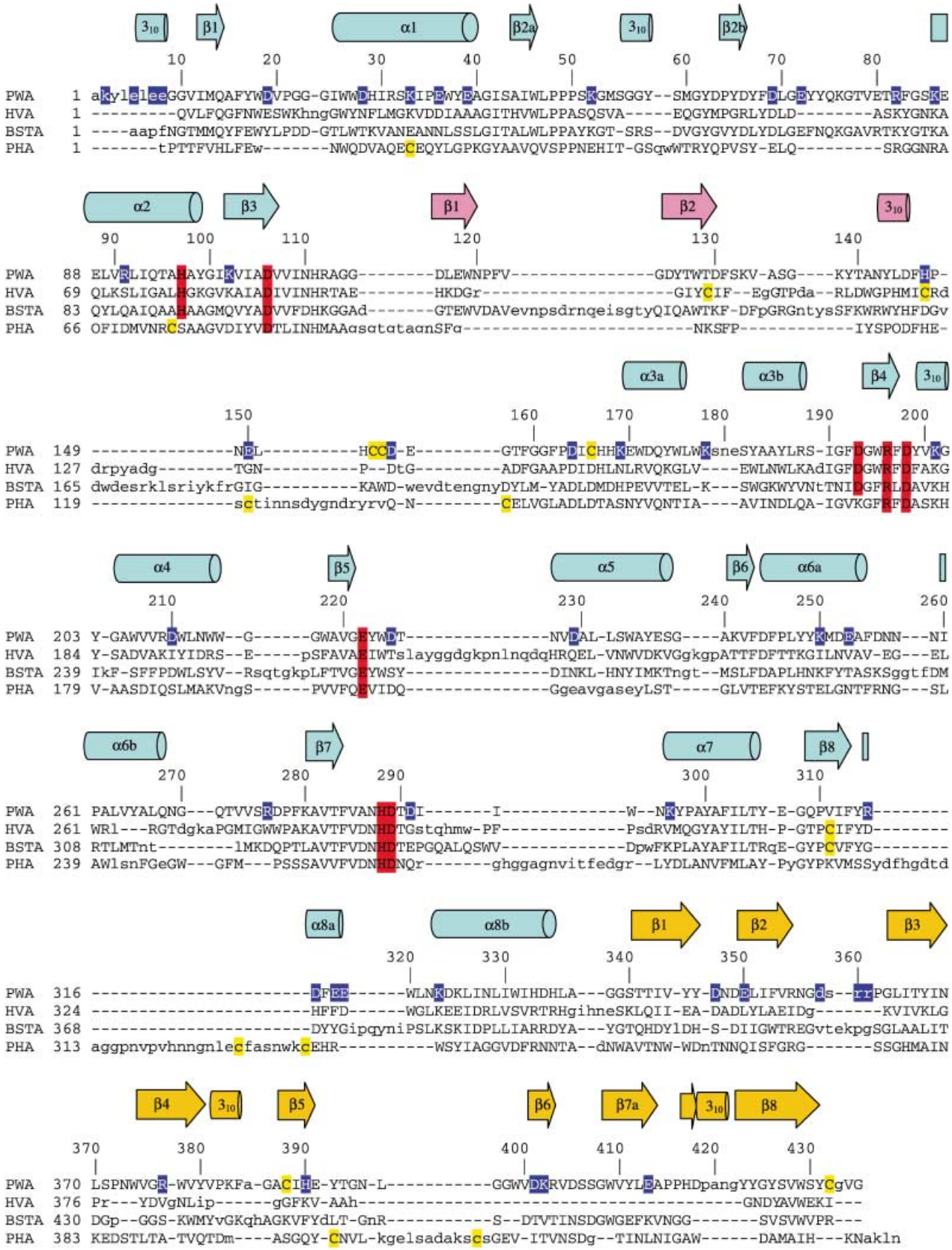

Figure 1. *Structure-based sequence alignment of α-amylase sequences, from the coordinates of the PWA, BSTA, HVA and PHA structures (see Methods). The secondary structure assignments are taken from the PWA structure.[19] The colouring scheme for domains A, B and C is cyan, magenta and orange, respectively. Helices are shown as cylinders, and β-strands are displayed as arrows. Residues involved in ion pairs are highlighted in blue, and those that are structurally conserved in at least three structures are shown in red. Cysteines are highlighted in yellow.*

Table 4. *Number and volumes of cavities in α-amylases.*

Enzyme	Total no. cavities	Total volume of cavities [Å^3]	Total area of cavities [Å^2]	Total protein volume [Å^3]	Total volume cavities/protein [%]
PWA	28	936.57	1541.27	46200	3.34
BSTA	44	1466.32	2395.25	50730	4.72
HVA	52	1698.69	2750.44	41550	6.61
PHA	38	1181.87	1902.74	44800	4.25

families gives credence to the notion that they represent general features of α-amylase structures.[16, 24] These observations are further validated by a recent engineering experiment in which the thermostability of BLA was increased considerably by converting a number of polar surface residues into apolar ones.[23] The crystal structure of the BLA mutant protein (PDB code: 1OB0) revealed that changes leading to an increase in the surface hydrophobicity of the protein might be complemented by improvements in the hydrophobic packing microenvironments near or at the protein surface. This may explain, in part, the apparent discrepancy between these data and those from previous engineering experiments.[25]

Salt bridges and salt bridge clusters

Comparative analysis of the four α-amylase structures reveals that, in general, an increase in the number of salt bridges is associated with an increase in the thermostability of the protein. Use of a subset of salt bridges believed to have a high impact on thermal stability (maximum distance, 3.5 Å; surface exposed salt bridges only)[13] indicates that the normalised ratio of salt bridges is over twice as high in BSTA as in PHA (5.0 and 2.2, respectively; see Table 5). These differences were most pronounced in the thermophilic BSTA and the psychrophilic PHA structures (Figure 2, Table 5), less dramatic differences being noted between the PWA and HVA structures. Overall, the data support a statistically significant positive correlation between an increase in the number of salt bridges and protein thermostability.[13, 14, 16] However, recent experimental and statistical data have provided support for the premise that the contributions of salt bridges to thermostability are critically dependent on their local environment and may, in fact, be enhanced by the formation of salt bridge networks.[13, 26] Further examination of certain salt bridges found in the α-amylases currently under investigation was undertaken in an effort to substantiate these findings.

The first example consists of the four-membered salt bridge cluster located in domain A of PWA. This domain is formed by a $(\beta\alpha)_8$-barrel made up of an inner parallel β-barrel and an outer parallel α-helical wheel. While the inner barrel is connected by a continuous parallel β-sheet hydrogen network, the helices of the outer α-helical ring are not connected by any systematic interaction pattern. The helix – helix interfaces originate from helices that are topologically adjacent and equally separated by 25 – 40 residues in sequence, except for the interface formed by the N-terminal helix α1 and the C-terminal helix pair α8a and α8b, separated by about 300 residues. In a related $(\beta\alpha)_8$-barrel fold from phosphoribosyl anthranilate isomerase, a stabilising salt bridge connecting helices α1 and α8 has been found in the protein structure of a hyperthermophilic representative *(T. maritima)*, while being absent in the structure from the mesophile *E. coli*.[27, 28] Indeed, the same interface of the $(\beta\alpha)_8$-barrel domain B of the PWA structure contains a four-membered salt bridge cluster (Figure 3) involving two residues from α-helix 1 (K33, E36) and two residues from the α-helix 8a/α-helix 8b segment (E318, K323). These four residues form a ring-like ion pair network in PWA, and according to the criteria of Xiao and Honig (1999),[13] this cluster should have a strong stabilising potential. Our comparison reveals that the complete cluster is not found in any of the other α-amylase structures. While in the mesophilic HVA structure there is still one salt bridge connecting helices α1 and α8b, matching the PWA-pattern (D28, K331), only one unrelated salt bridge cluster (E19, R338; E19, H337) is found in the same interface of the psychrophilic PHA structure. In this latter structure, however, the α-helix 8a/α-helix 8b segment is preceded by a 30-residue hydrophilic loop (Figure 1), which may confer a different function on this salt bridge. In the thermophilic BSTA structure, the α1 – α8 interface is devoid of any salt bridges. However, the overall high number of salt bridges found in BSTA may indicate in general that it may have acquired its observed thermostability independently (Table 5). Although the precise molecular basis for the involvement of the PWA salt bridge cluster in PWA hyperthermostability so far remains elusive, there is speculation with respect to its role in PWA folding. If this ion pair cluster is formed in the early stages of the folding process, leading to a ring-like precursor fold, the entropic cost of associating structural elements at remote locations in the amino acid sequence would be reduced, leading to temperature-dependent relative energetic stabilisation of the folded state

Table 5. *Salt bridges ≤ 4.0 (≤ 3.5 Å).*

Name	Total number of salt bridges	Salt bridges per residue [%]	Number of surface salt bridges	Surface salt bridges per residue [%]
PWA	33 (26)	7.6 (6.0)	22 (16)	5.1 (3.7)
BSTA	40 (35)	8.3 (7.2)	25 (24)	5.2 (5.0)
HVA	28 (22)	6.9 (5.5)	21 (14)	5.2 (3.5)
PHA	24 (20)	5.3 (4.4)	13 (10)	2.9 (2.2)

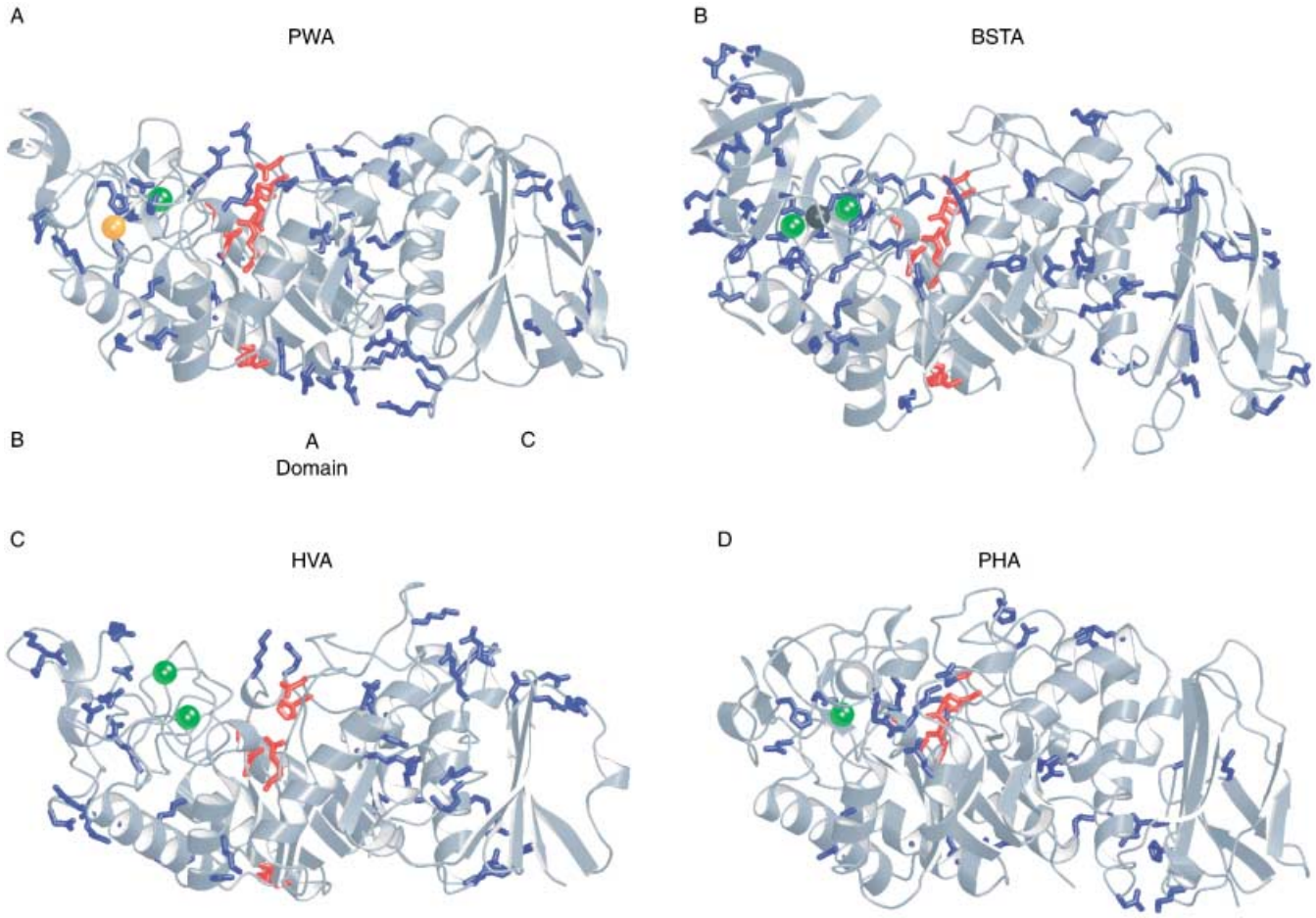

Figure 2. *Salt bridge distribution in the α-amylase structures PWA (A), BSTA (B), HVA (C) and PHA (D) (cf. Table 5). Those residues involved in salt bridges and conserved in at least three structures are in red, others are in blue. The positions of the metal centres are depicted by green (Ca) and orange spheres (Zn). The domain structure of PWA (A, B, C) is indicated and is similar to that of the other α-amylase structures used for comparison.*

with regard to the suggested precursor state. In fact, a disulfide bridge-containing analogue of phosphoribosyl anthranilate isomerase $(\beta\alpha)_8$-barrel from yeast, producing a ring-like structure of the unfolded state, did lead to a stabilisation of the folded state.[29]

The second example involves salt bridges found in the vicinity of the conserved α-amylase calcium site.[30] In the structure of PWA, helix α3 of the $(\beta\alpha)_8$-barrel domain A is split into two parts separated by a short loop. This loop is consistently found in the sequences of the archaeal *Thermococcales* order, but is not present in the sequences of the other three α-amylase structures used for comparison. The first residue of this loop (K178) is involved in a salt bridge with D210 from helix α4 (Figure 4). In the thermophilic BSTA structure, there is a salt bridge in a similar position (K216, D246). In contrast, in the HVA and PHA structures, there is no salt bridge connecting these two helices. In addition, in PWA, there is a salt bridge connecting the helix α3a and the loop connecting domains A and B (E150, K169), while in BSTA a similar salt bridge (E210, H160) connects helix α3 and the 3_{10}-helix preceding the fourth β-strand of domain B. Again, no comparable ion pair is present in the other two α-amylase structures. It is notable that both salt bridges (K178 – D210; E150 – K169) link sequence elements in proximity to the PWA-specific (Ca, Zn) metal binding site, possibly contributing to its structural integrity and stability, which appears to be a major determinant of thermostability in α-amylases (see below).

The third example of a salt bridge involves a specific structure in the N terminus of PWA, not found in the other three α-amylase structures compared here (Figure 5). This region includes an ion pair cluster formed by the N-terminal amino groups of A1, E5, E7 and K102. More specific interactions to other parts of PWA are provided by K2 and E8. A similar salt bridge is found in *Thermotoga maritima* indoleglycerol phosphate synthase (tIGPS), fixing the N terminus to the protein core and thereby stabilising the overall structure.[27]

Cysteines

The sequences of the four α-amylases compared in this contribution contain one to eight cysteines, with no apparent association between this number and their observed thermostabilities (Table 6, Figure 6). In the PWA structure, four of the five cysteine residues are involved in disulfide bridges.[19] The C153 – C154 bridge is located in domain B in the vicinity of the PWA-

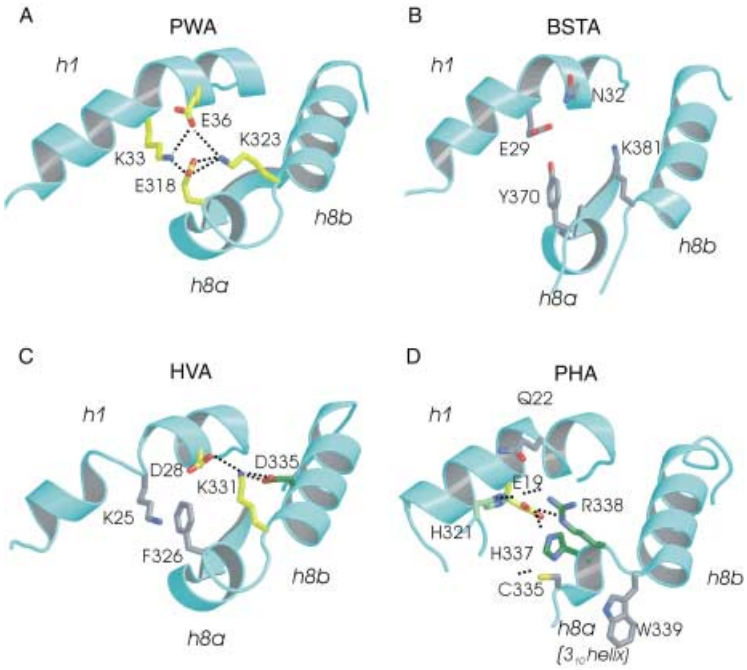

Figure 3. *Ion pairs between helix α1 and helix α8 of the $(\beta\alpha)_8$-barrel domain A. A: PWA. B: BSTA. C: HVA. D: PHA. In PWA, there is an ion pair cluster formed by two negatively charged and two positively charged residues; the same residues are shown in the other three structures. Their carbon backbone appears in yellow if engaged in equivalent salt bridges, otherwise in grey. Structurally unrelated salt bridges are in green. Ion pairs with distances ≤ 4 Å are shown by dashed lines.*

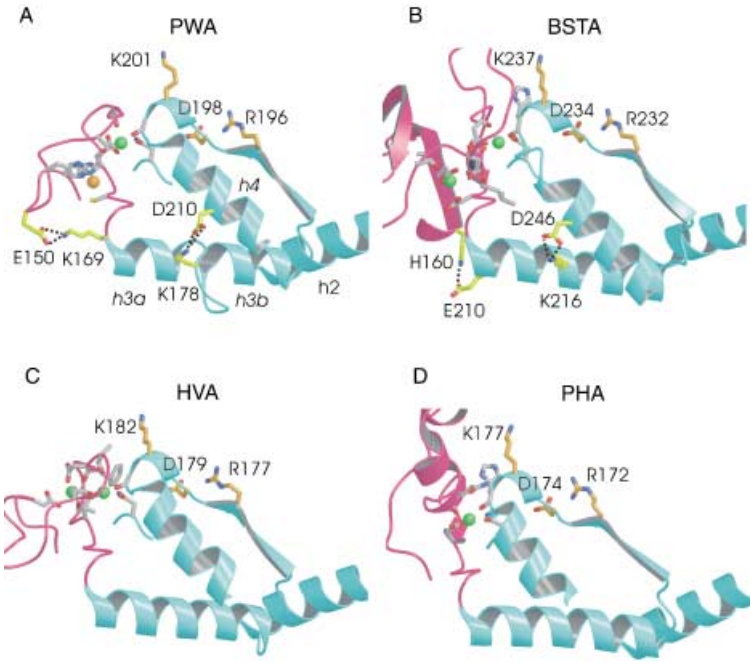

Figure 4. *Active site and metal binding site stabilisation by salt bridges in PWA (A), BSTA (B), HVA (C) and PHA (D). Carbon atoms from side chain residues forming salt bridges are coloured yellow. Those involved in active site substrate binding and metal coordination are in orange and grey, respectively. For the sake of clarity, not all active site and metal binding site residues are depicted. Bound ions are shown in green (calcium), dark grey (sodium) and orange (zinc). The ribbon colours are as in Figure 1.*

Table 6. *Number of cysteines and disulfide bridges.*

Name	Total number of cysteines	Number of disulfide bridges	Specific functions
PWA	5	2	C166: binding to (Ca, Zn) site
BSTA	1	0	
HVA	3	0	
PHA	8	4	

specific (Ca, Zn) di-metal binding site. It crosslinks two neighbouring residues, a rare feature in protein structures. The second disulfide bridge is located in domain C. The only cysteine (C166) not involved in disulfide bridge formation serves as one of the coordinating ligands of the PWA (Ca, Zn) metal binding site. Primary sequence analysis revealed that, while the two cysteines contributing to the disulfide bridge in domain C are conserved among archaeal *Thermococcales* sequences (but not in other α-amylase sequences), the disulfide bridge between C153 and C154 and C166 is found only in some members of the order *Thermococcales* (data not shown). In a previous site-directed mutagenesis study, while the contribution of the first four cysteines to thermostability was found to be insignificant, replacement of C166 by serine nonetheless led to loss of thermostability,[31] indirectly suggesting a role of the (Ca, Zn) di-metal site in thermostability (see below). On the other hand, the only cysteine found in the BSTA sequence would be expected to be deprotonated, and as such appears to be a major cause for thermal inactivation under high-pH conditions,[32] While all eight cysteines in PHA are involved in disulfide bridge formation, no disulfide bridges are found in the HVA structure.

Overall, comparison of the four α-amylase structures reported on in this contribution reveals no apparent association between disulfide bridge formation and protein thermostability. Although the presence of disulfide bridges may provide an entropic advantage in protein folding,[33] cysteine and/or cystine residues are particularly prone to chemical degradation at high temperatures.[33] In specific cases such as, for example, the involvement of C166 in metal binding in PWA, the presence of cysteines may contribute to thermal stabilisation.

Specific two-metal centres as markers for thermostability

The known class-13 α-amylase structures share a common calcium binding site located in the interface of domains A and B in close proximity to the active site (Figures 4 and 7). This site appears to be essential for structural integrity and catalytic activity of the protein.[18] The coordination geometry of this calcium site

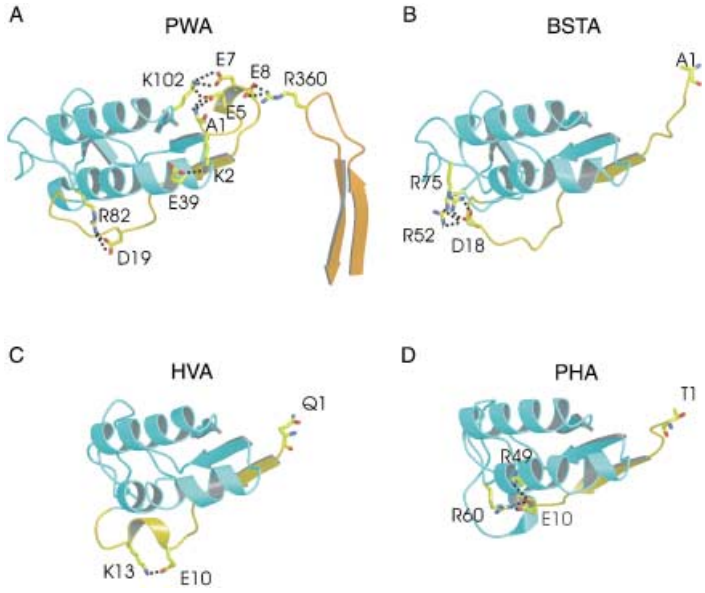

Figure 5. *Anchoring of the N terminus and stabilisation of the N-terminal region by salt bridges in PWA. The extended N terminus of domain A residues is in yellow. Otherwise, the colouring Scheme of Figure 1 has been applied.*

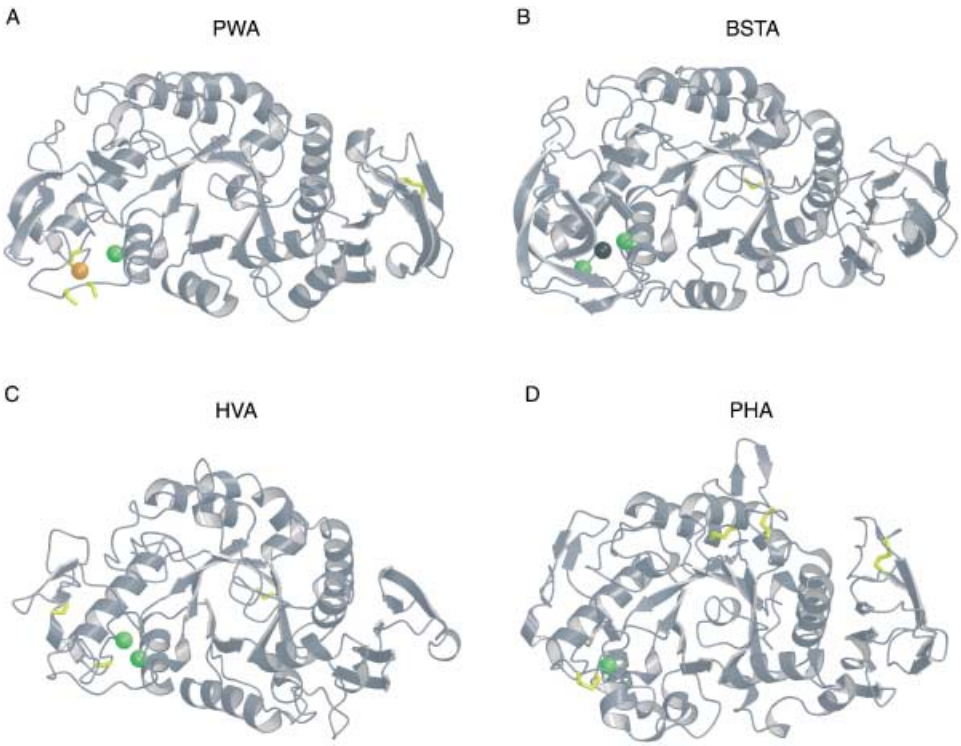

Figure 6. *Cysteines and disulfide bridges in PWA (A), BSTA (B), HVA (C) and PHA (D) (cf. Table 6). The metal ions are coloured as in Figure 4. Cysteines and disulfide bridges are in yellow.*

is highly conserved in α-amylases, irrespective of their origin. However, while the calcium ion is pentacoordinated by protein residues in the structures of PWA, BSTA and HVA, in the cold-adapted PHA structure, only four protein ligands bind calcium.

In addition, representative thermophilic and mesophilic/psychrophilic structures exhibit important differences with respect to the presence of a second metal binding site close to the conserved calcium binding site. In PWA, the second site is occupied by zinc, as shown by X-ray crystallography and PIXE analysis (Figure 7 a).[19, 31] Replacement of one of its ligands (C166) leads to loss of PWA hyperthermostability.[31] Treatment with compounds such as DTT or EDTA at room temperature does not lead to significant reductions in the catalytic activity and hyperthermostability of PWA, indicating tight binding of the two metal ions.[19, 31] These data may also provide an explanation as to why PWA, unlike many other α-amylases, does not require the addition of exogenous calcium for full catalytic activity.[34, 35]

A different type of di-metal centre has been observed in the structures of BLA and BSTA, in which second calcium ions are found at distances of 8.5 and 8.7 Å, respectively, from the conserved calcium binding site (Figure 7 b). In contrast to the di-metal (Ca, Zn) site in PWA, the (Ca, Ca) site in BSTA and in BLA is bridged by a sodium ion.[36, 37] This site was first postulated to play a role in the thermostability of BLA, and this was later confirmed experimentally.[23, 36, 38]

Comparison of the di-metal centres in PWA and BSTA (Figure 7 e) reveals that they appear to have evolved independently. Both di-metal centres are highly sequence-specific and are found only in thermostable close homologues, indicating late emergence. The presence of the highly conserved calcium binding site supports the idea of a common origin for all family-13 amylases. The second metal binding site present in some thermostable α-amylases prompts the assumption that an evolutionary process for environmental adaptation has evolved α-amylases containing a structurally similar di-metal centre with different metal specificities. This argument is further supported by the absence of this second binding site in the mesophilic/psychrophilic α-amylase structures used for comparison.

Conclusion

Thanks to the abundance of functional and structural data, class-13 α-amylases serve as good targets for analysis of both general and specific molecular parameters that may promote protein thermostability. This comparison, restricted to four representative structures, supports previously identified general trends, such as an increase in salt bridges to

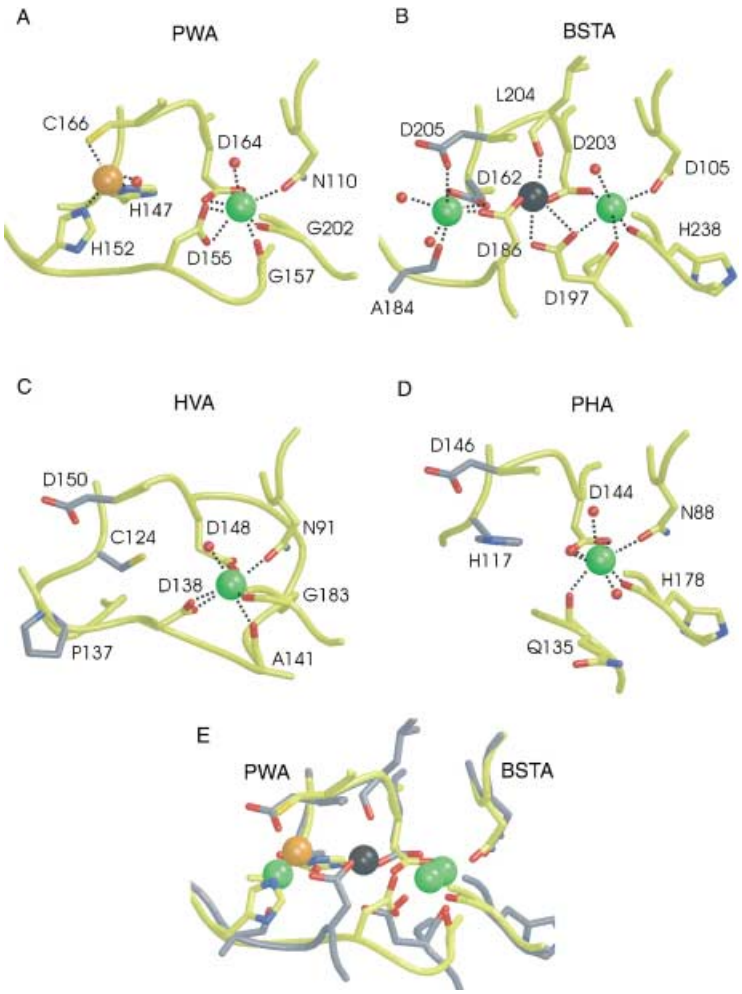

Figure 7. *Close-up view of the highly conserved calcium binding site in PWA (A), BSTA (B), HVA (C) and PHA (D). The ions are coloured as in Figure 4, ordered solvent molecules are shown in red. Carbon atoms are in yellow, except for those from side chain residues superimposable with the zinc coordinating residues of PWA, which are grey. E: Superposition of the (Ca, Zn) two-metal binding site of PWA (yellow) with the Ca-Na-Ca metal triad of BLA (grey). Water molecules involved in metal coordination are not depicted.*

improve thermostability. Our study also shows, through direct comparison of representative bacterial and archaeal structures (PWA, BSTA), that molecular parameters possibly contributing to thermostability are not conserved across proteins from different organisms living in an elevated-temperature environment. Therefore, we postulate that thermal adaptation—at least in these examples—may have emerged during late stages of evolution, in contrast to protein function. The observation is particularly true for the di-metal centres in the thermophilic PWA and BLA/BSTA structures. Although they seem to serve the same purpose—thermostabilisation of the active site architecture—they have evolved independently, emerging into distinct (Ca, Zn) and (Ca, Na, Ca) binding sites.

Computational methods

The Secondary Structure Matching (SSM) server of the Macromolecular Structure Database (EBI-MSD at http://www.ebi.ac.uk/msd-srv/ssm) was used for selection of family-13 α-amylase structures. Structures were superimposed on the basis of the rotation and translation matrices obtained by the SSM server and visualised with the program PyMOL Molecular Graphic System, version 0.86.[39] The resulting structural alignment was used for direct sequence comparisons. Primary sequence alignment was performed with WU-BLAST[40] (http://www.ebi.ac.uk/blast2).

The total volumes of the enzymes were calculated with the aid of VOIDOO.[41] Structural cavities were identified and the volumes were calculated with a probe radius of 1.4 Å by using the CASTp server[42] (http://cast.engr.uic.edu/cast). The solvent-accessible surface area/volume ratios were calculated with the program GRASP,[43] with use of a probe radius of 1.4 Å. HETATOM records and hydrogen atoms, when present, were not used in these calculations. The program GETAREA 1.1 was used[44] (http://www.scsb.utmb.edu/cgi-bin/get a form.tcl) to define and calculate the solvent accessibility per residue used in the assignment of solvent exposure of salt bridges. The distribution of apolar and polar accessible surface areas (ASA) was calculated with aid of the program Sracer,[45] with use of a probe radius of 1.4 Å.

The overall number of salt bridges was calculated by using the protein verification tools of the WHAT IF suite 5.0, WHAT CHECK.[46] Salt bridges were categorised as solvent-exposed through application of a previously published scheme.[47] Each salt bridge formed by two side chain residues with more than one charged atom involved was counted only once.

Keywords: α-amylase · glycoside hydrolase family-13 · metal binding · salt bridge · thermostability

[1] C. R. Woese, G. E. Fox, *Proc. Natl. Acad. Sci. USA* **1977**, *74*, 5088 – 5090.
[2] C. R. Woese, O. Kandler, M. L. Wheelis, *Proc. Natl. Acad. Sci. USA* **1990**, *87*, 4576 – 4579.
[3] H. Huber, K. O. Stetter, *J. Biotechnol.* **1998**, *64*, 39 – 52.
[4] R. M. Daniel, D. A. Cowan, H. W. Morgan, M. P. Curran, *Biochem. J.* **1982**, *207*, 641 – 644.
[5] R. M. Daniel, M. Dines, H. H. Petach, *Biochem. J.* **1996**, *317*(1), 1 – 11.
[6] E. Pennisi, *Biotechnology* **1997**, *176*, 705 – 706.
[7] M. W. Adams, R. M. Kelly, *Bioorg. Med. Chem.* **1994**, *2*, 659 – 667.
[8] A. Persidis, *Nat. Biotechnol.* **1998**, *16*, 593 – 594.
[9] C. Bertoldo, G. Antranikian, *Curr. Opin. Chem. Biol.* **2002**, *6*, 151 – 160.
[10] M. J. van der Maarel, B. van der Veen, J. C. Uitdehaag, H. Leemhuis, L. Dijkhuizen, *J. Biotechnol.* **2002**, *94*, 137 – 155.
[11] R. Sterner, W. Liebl, *Crit. Rev. Biochem. Mol. Biol.* **2001**, *36*, 39 – 106 and references therein.
[12] C. Vieille, J. G. Zeikus, *Microbiol. Mol. Biol. Rev.* **2001**, *65*, 1 – 43 and references therein.
[13] L. Xiao, B. Honig, *J. Mol. Biol.* **1999**, *289*, 1435 – 1444.
[14] A. Szilagyi, P. Zavodsky, *Structure* **2000**, *8*, 493 – 504.
[15] S. Kumar, R. Nussinov, *Cell. Mol. Life Sci.* **2001**, *58*, 1216 – 1233.
[16] G. Gianese, F. Bossa, S. Pascarella, *Proteins* **2002**, *47*, 236 – 249.
[17] B. Henrissat, A. Bairoch, *Biochem. J.* **1996**, *316*, 695 – 696.
[18] S. Janecek, *Prog. Biophys. Mol. Biol.* **1997**, *67*, 67 – 97 and references therein.

[19] A. Linden, O. Mayans, W. Meyer-Klaucke, G. Antranikian, M. Wilmanns, *J. Biol. Chem.* **2003**, *278*, 9875 – 9884.
[20] N. Aghajari, G. Feller, C. Gerday, R. Haser, *Structure* **1998**, *6*, 1503 – 1516.
[21] J. Fitter, R. Herrmann, N. A. Dencher, A. Blume, T. Hauss, *Biochemistry* **2001**, *40*, 10723 – 10731.
[22] N. Declerck, M. Machius, P. Joyet, G. Wiegand, R. Huber, C. Gaillardin, *Protein Eng.* **2003**, *16*, 287 – 293.
[23] M. Machius, N. Declerck, R. Huber, G. Wiegand, *J. Biol. Chem.* **2003**, *278*, 11546 – 11553 and references therein.
[24] J. J. Tanner, R. M. Hecht, K. L. Krause, *Biochemistry* **1996**, *35*, 2597 – 2609.
[25] R. Jaenicke, G. Boehm, *Curr. Opin. Struct. Biol.* **1998**, *8*, 738 – 748 and references therein.
[26] C. Vetriani, D. L. Maeder, N. Tolliday, K. S. P. Yip, T. J. Stillman, K. L. Britton, D. W. Rice, H. H. Klump, F. T. Robb, *Proc. Natl. Acad. Sci. USA* **1998**, *95*, 12300 – 12305.
[27] A. Merz, T. Knochel, J. N. Jansonius, K. Kirschner, *J. Mol. Biol.* **1999**, *288*, 753 – 763.
[28] M. Wilmanns, J. P. Priestle, T. Niermann, J. N. Jansonius, *J. Mol. Biol.* **1992**, *223*, 477 – 507.
[29] J. Eder, M. Wilmanns, *Biochemistry* **1992**, *31*, 4437 – 4444.
[30] E. Boel, L. Brady, A. M. Brzozowski, Z. Derewenda, G. G. Dodson, V. J. Jensen, S. B. Petersen, H. Swift, L. Thim, H. F. Woldike, *Biochemistry* **1990**, *29*, 6244 – 6249.
[31] A. Savchenko, C. Vieille, S. Kang, J. G. Zeikus, *Biochemistry* **2002**, *41*, 6193 – 6201.
[32] S. J. Tomazic, A. M. Klibanov, *J. Biol. Chem.* **1988**, *263*, 3086 – 3091.
[33] T. A. Klink, K. J. Woycechowsky, K. M. Taylor, R. T. Raines, *Eur. J. Biochem.* **2000**, *267*, 566 – 572.
[34] G. Dong, C. Vieille, A. Savchenko, J. G. Zeikus, *Appl. Environ. Microbiol.* **1997**, *63*, 3569 – 3576.
[35] S. Jorgensen, C. E. Vorgias, G. Antranikian, *J. Biol. Chem.* **1997**, *272*, 16335 – 16342.
[36] M. Machius, N. Declerck, R. Huber, G. Wiegand, *Structure* **1998**, *6*, 281 – 292.
[37] D. Suvd, Z. Fujimoto, K. Takase, M. Matsumura, H. Mizuno, *J. Biochem. (Tokyo)* **2001**, *129*, 461 – 468.
[38] N. Declerck, M. Machius, G. Wiegand, R. Huber, C. Gaillardin, *J. Mol. Biol.* **2000**, *301*, 1041 – 1057.
[39] W. L. DeLano, *The PyMOL Molecular Graphics System*, DeLano Scientific LLC, San Carlos, CA, USA.
[40] S. F. Altschul, T. L. Madden, A. A. Schaffer, J. Zhang, Z. Zhang, W. Miller, D. J. Lipman, *Nucleic Acids Res.* **1997**, *25*, 3389 – 3402.
[41] G. J. Kleywegt, T. A. Jones, *Acta Crystallogr. Sect. D: Biol. Crystallogr.* **1994**, *50*, 178 – 185.
[42] J. Liang, H. Edelsbrunner, C. Woodward, *Protein Sci.* **1998**, *7*, 1884 – 1897.
[43] A. Nicholls, K. Sharp, B. Honig, *Proteins* **1991**, *11*, 281 – 296.
[44] R. Fraczkiewicz, W. Braun, *J. Comput. Chem.* **1998**, *19*, 319 – 333.
[45] O. V. Tsodikov, M. T. Record, Jr., Y. V. Sergeev, *J. Comput. Chem.* **2002**, *23*, 600 – 609.
[46] R. Rodriguez, G. Chinea, N. Lopez, T. Pons, G. Vriend, *CABIOS Comput. Appl. Biosci.* **1998**, *14*, 523 – 528.
[47] S. Kumar, B. Ma, C.-J. Tsai, R. Nussinov, *Proteins: Struct. Funct. Genet.* **2000**, *38*, 383 – 397.
[48] E. Bertoft, C. Andtfolk, S.-E. Kulp, *J. Inst. Brew.* **1984**, *90*, 298 – 302.
[49] S. D'Amico, C. Gerday, G. Feller, *J. Biol. Chem.* **2002**, *277*, 46110 – 46115.

Received: August 4, 2003 [F 734]

